

## LETTER

### Network-forming Ni in silicate glasses

LAURENCE GALOISY,\* GEORGES CALAS

Laboratoire de Minéralogie-Cristallographie, URA CNRS 09, Universités de Paris 6 et 7 and IPGP, 75252 Paris Cedex 05, France

#### ABSTRACT

NiK-edge EXAFS and XANES and optical spectroscopy indicate strong differences in the Ni environments in glasses of feldspar stoichiometry, in relation to the polarizing power of the associated alkali. Mostly  $^{64}\text{Ni}$  and coexisting  $^{65}\text{Ni}$  and  $^{60}\text{Ni}$  are found in  $\text{K}_2\text{NiSi}_3\text{O}_8$  and  $\text{Na}_2\text{NiSi}_3\text{O}_8$  glasses, respectively. The  $^{64}\text{Ni}$  belongs to the silicate network with Ni-O-Si angles of  $127 \pm 5^\circ$ . Si-O-T angles decrease in silicate glasses with the decreasing charge of the tetrahedral cation T. The distribution of Ni between two sites in silicate glasses and melts may strongly influence the chemical dependence of partition coefficients for Ni between mineral and liquid.

#### INTRODUCTION

The interpretation of the abundance and distribution of trace elements in magmatic systems requires the precise knowledge of partition coefficients between mineral and liquid. However, the chemical dependence of these coefficients limits the quantitative modeling of magmatic differentiation processes. The influence of melt structure and composition on partition coefficients has been clearly demonstrated in most natural and synthetic systems (Lemarchand et al., 1987; Kinzler et al., 1990). Among the trace elements commonly studied, Ni has large olivine-melt distribution coefficients,  $D^{\text{Ni}}$ , which make it a useful tracer to determine the petrogenetic history of mafic and ultramafic magmas (Hart and Davis, 1978). Recent spectroscopic studies have shown the presence of  $^{65}\text{Ni}$  in glassy  $\text{CaNiSi}_2\text{O}_6$  (Galoisy and Calas, 1991). This unusual coordination state is found in most oxide glasses (Galoisy and Calas, in preparation) but is rather rare in crystalline compounds that contain mostly  $^{60}\text{Ni}$  and  $^{64}\text{Ni}$ . Although Ni is considered as a typical network modifier (Nelson et al., 1983), a minor amount of  $^{64}\text{Ni}$  has also been recognized in silicate glasses (Burns and Fyfe, 1964; Calas and Petiau, 1983; Galoisy and Calas, 1991). However, its structural significance has never been clarified.

We present in this paper spectroscopic evidence for  $^{64}\text{Ni}$  in glasses with compositions close to  $\text{K}_2\text{NiSi}_3\text{O}_8$  and  $\text{Na}_2\text{NiSi}_3\text{O}_8$ . The Ni coordination state is deduced from optical absorption spectroscopy and X-ray absorption near-edge structure (XANES) as well as from the short Ni-O distances derived from extended X-ray absorption

fine-structure (EXAFS). Such important changes in the coordination number provide information about the origin of the chemical dependence of  $D^{\text{Ni}}$  (Kinzler et al., 1990). The interpretation of Ni playing a network-forming role relies on the well-defined structural relationships of  $\text{NiO}_4$  tetrahedra with the silicate network. The Si-O- $^{64}\text{Ni}$  angle is the smallest of the intertetrahedral angles measured in silicate glasses. Together with the presence of mostly  $^{65}\text{Ni}$  in K-free silicate glasses (Galoisy and Calas, in preparation), these data predict coordination changes of Ni in magmatic liquids at high pressure as in their ferrous counterparts (Waychunas et al., 1988).

#### EXPERIMENTAL

The glasses were synthesized from reagent-grade component oxides and carbonates by melting in Pt crucibles at 1350 °C for 24 h, crushing the resulting glass to ensure homogeneity, remelting at 1550 °C for 2 h, and quenching in  $\text{H}_2\text{O}$ . The resulting glass was crystal free, optically isotropic, and X-ray amorphous. The potassic and the sodic glasses had distinct coloration, deep purple and dark brown, respectively. Electron microprobe analyses indicated chemically homogeneous glasses with the following stoichiometries:  $\text{Na}_{2.07}\text{Ni}_{0.95}\text{Si}_{2.98}\text{O}_8$  and  $\text{K}_{1.90}\text{Ni}_{0.99}\text{Si}_{3.02}\text{O}_8$ .

Optical diffuse reflectance spectra were obtained from 250 to 2500 nm using a computerized 2300 Cary spectrophotometer fitted with an integrating sphere attachment coated with halon. Reflectance spectra, obtained by reference to halon, were converted into a remission function  $F(R)$ , as an approximation of sample absorbance (Galoisy et al., 1991).

NiK-edge XAS transmission spectra of finely ground powders were recorded at room temperature and 77 K on D1 and D4 stations at the LURE DCI Synchrotron

\* Present address: CHiPR and Department of Earth and Space Sciences, State University of New York, Stony Brook, New York 11794, U.S.A.

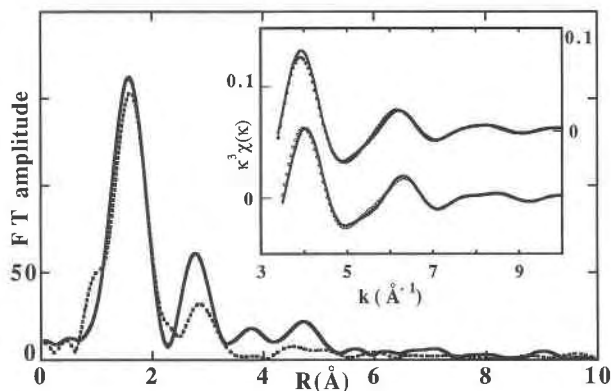


Fig. 1. Fourier transforms of  $k^3$ -weighted NiK-EXAFS spectra of  $K_2NiSi_3O_8$  (solid line) and  $Na_2NiSi_3O_8$  (dashed line) glasses. Inset: experimental (solid line) and calculated (points) EXAFS functions corresponding to Ni-O and Ni-Si contributions for  $K_2NiSi_3O_8$  (open circles, lower curve) and  $Na_2NiSi_3O_8$  (solid circles, upper curve) glasses.

Radiation Facility (Orsay, France). The storage ring was operated at 1.85 GeV positron energy and 250 mA positron current. Si (111) and Si (311) two-crystal monochromators were used for EXAFS and XANES, respectively, with an energy resolution of about 1.4 eV for XANES. The spectra were calibrated by reference to metallic Cu. Data reduction was initiated using least square iteration, according to a procedure previously described (Galoisy and Calas, 1991). Theoretical phase shift and amplitude functions have been used (McKale et al., 1988), and the EXAFS fitting parameters were checked by reference to crystalline  $NiCr_2O_4$  and  $CaNiSi_2O_6$ , the mean free path parameter,  $\lambda$ , being kept at 1.7 Å. The accuracy of  $d(Ni-O)$  and  $d(Ni-Si)$  distances and Ni coordination number ( $N$ ) was 0.01 Å, 0.03 Å, and 0.5, respectively.

## RESULTS

The NiK-edge EXAFS spectra of the two glasses extend up to  $10.5 \text{ \AA}^{-1}$  and show significant differences, which are visualized on the Fourier transform (FT) (Fig. 1). As compared to the sodic glass, the FT corresponding to the potassic glass shows a shift of the Ni-O peak toward lower values and a more intense second peak. EXAFS-derived Ni-O distances and coordination number,  $N$ , are  $d(Ni-O) = 1.99 \text{ \AA} \pm 0.01 \text{ \AA}$  and  $1.96 \text{ \AA} \pm 0.01 \text{ \AA}$ , and  $N = 4.2 \pm 0.5$  and  $3.8 \pm 0.5$ , for the  $Na_2NiSi_3O_8$  and  $K_2NiSi_3O_8$  glasses, respectively. The Debye-Waller type factor,  $\sigma$ , is larger in the  $Na_2NiSi_3O_8$  glass than in the  $K_2NiSi_3O_8$  glass,  $\sigma = 0.094$  and  $0.085 \text{ \AA}$ , respectively. These values remain lower than the upper  $\sigma$  limit ( $\sigma = 0.14 \text{ \AA}$ ) for the Ni-O distance distribution described in a harmonic approximation (Eisenberger and Brown, 1979). Similar EXAFS parameters have been found for  $^{51}Ni$  in  $CaNiSi_2O_6$  glass [ $d(Ni-O) = 1.98 \text{ \AA}$  and  $N = 4.5$ ] (Galoisy and Calas, 1991). Thus, EXAFS data alone cannot decipher unambiguously between fourfold and fivefold coordination. The second peak is modeled with Si atoms as second neigh-

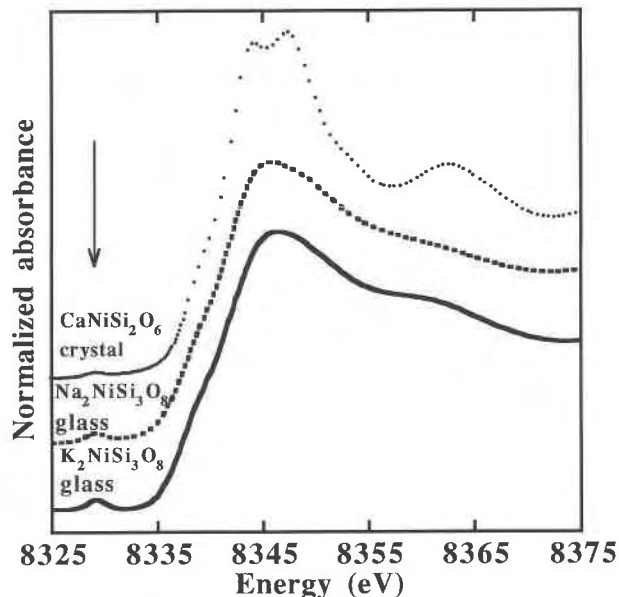


Fig. 2. NiK-XANES spectra of  $K_2NiSi_3O_8$  and  $Na_2NiSi_3O_8$  glasses compared with the NiK-XANES spectrum of crystalline  $CaNiSi_2O_6$ . The arrow indicates the position of the preedge.

bors:  $d(Ni-Si) = 3.23$  and  $3.19 \text{ \AA} (\pm 0.01 \text{ \AA})$ ,  $N = 1.7$  and  $4 (\pm 0.5)$ , and  $\sigma = 0.1$  for the sodic and the potassic glass, respectively (see inset of Fig. 1). The upper limit of the  $\sigma$  values for the Ni-Si contribution described in a harmonic approximation is  $0.18 \text{ \AA}$ , which validates our analysis. Even at low temperature, no contribution from alkalis has been detected.

The NiK-XANES features of the  $Na_2NiSi_3O_8$  glass such as preedge intensity, shape, and intensity of the edge crest (Fig. 2) are intermediate between those found for  $^{60}Ni$  and  $^{40}Ni$  in crystalline compounds, as already observed in the  $CaNiSi_2O_6$  glass (Galoisy and Calas, 1991). The preedge is more intense in the  $K_2NiSi_3O_8$  glass and is similar to that measured in  $NiCr_2O_4$  (Manceau and Calas, 1986). This indicates that an inversion center is lacking at the Ni site in the potassic glass (Calas and Petiau, 1983). Together with the low intensity of the edge crest, which indicates tetrahedral coordination (Cartier and Verdaguier, 1989), the NiK-XANES spectrum of  $K_2NiSi_3O_8$  glass corresponds to mostly  $^{40}Ni$ .

The distinct glass coloration comes from a modification of the Ni absorption bands (Fig. 3). The five major absorption bands observed in the  $K_2NiSi_3O_8$  glass correspond to the characteristic transitions of  $^{40}Ni$ , at  $5000 \text{ cm}^{-1}$  [ $^3T_1(F) \rightarrow ^3A_2(F)$ : crystal field splitting  $\Delta$ ],  $8300 \text{ cm}^{-1}$  [ $^3T_1(F) \rightarrow ^3T_2(F)$  transition], and  $15500$ ,  $17200$ , and about  $20000 \text{ cm}^{-1}$  [ $^3T_1(F) \rightarrow ^3T_1(P)$  transition split by the site distortion]. The sharp peak at  $13000 \text{ cm}^{-1}$  is diagnostic of the spin-forbidden  $^3T_1(F) \rightarrow ^1E(D)$  transition. This field-independent transition depends only on B and C Racah parameters, and its sharpness indicates no distribution of the Ni-O bond covalence (Burns, 1970). A minor proportion of  $^{51}Ni$  causes the absorption around  $22000 \text{ cm}^{-1}$ .

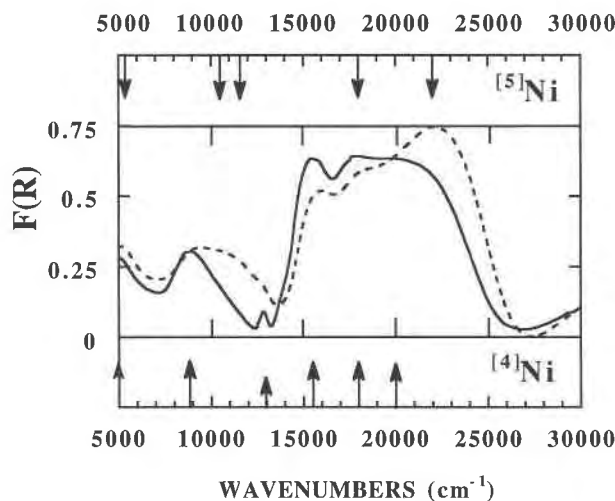


Fig. 3. Remission functions extracted from diffuse reflectance spectra of  $K_2NiSi_3O_8$  (solid line) and  $Na_2NiSi_3O_8$  glasses (dashed line). The transitions corresponding to  $^{55}Ni$  and  $^{64}Ni$  are indicated on the top and bottom, respectively.

Clearly,  $^{64}Ni$  is the major Ni species in the  $K_2NiSi_3O_8$  glass and occurs in a well-defined surrounding. The optical absorption spectrum of the  $Na_2NiSi_3O_8$  glass has quite a different shape, although the position of some bands remains the same (Fig. 4). Five main absorption bands are observed, some of which correspond to transitions assigned to  $^{55}Ni$  in  $CaNiSi_2O_6$  glass (Galoisy and Calas, 1991):  ${}^3E'(F) \rightarrow {}^3E''(F)$  at approximately  $5200\text{ cm}^{-1}$ ,  ${}^3E'(F) \rightarrow {}^3A'_2(F)$  and  ${}^3E'(F) \rightarrow {}^3A''_1, {}^3A'_2(F)$  poorly resolved near  $10500$  and  $11700\text{ cm}^{-1}$ , and the most intense,  ${}^3E'(F) \rightarrow {}^3A'_2(P)$  near  $22000\text{ cm}^{-1}$ . The weak  ${}^3E'(F) \rightarrow {}^3E'(P)$  transition of  $^{55}Ni$  expected near  $18000\text{ cm}^{-1}$  is hidden by the  ${}^3T_1(F) \rightarrow {}^3T_1(P)$  split transition of  $^{64}Ni$  at  $15700\text{ cm}^{-1}$  and  $18000\text{ cm}^{-1}$ , at the same position as in the  $K_2NiSi_3O_8$  glass. The two other transitions expected for  $^{64}Ni$  occur in the broad bands near  $10000\text{ cm}^{-1}$  and  $5200\text{ cm}^{-1}$ . Thus, despite the similar composition of the glasses, the local structure around Ni is clearly different and indicates a strong sensitivity of Ni to the nature of the alkali.

## DISCUSSION

Spectroscopic data on  $K_2NiSi_3O_8$  glass indicate the presence of mostly  $^{64}Ni$ . The Ni-O distance and crystal field parameters,  $\Delta = 5000\text{ cm}^{-1}$  and  $B = 714\text{ cm}^{-1}$ , are typical for  $^{64}Ni$  and are similar to those found in  $^{64}Ni$ -bearing spinels (Sakurai et al., 1969; Galoisy et al., 1991). Larger Ni-O distances and distinct site symmetry indicate a mixing of  $^{55}Ni$  and  $^{64}Ni$  in  $Na_2NiSi_3O_8$  glass, as was previously described in  $CaNiSi_2O_6$  glass (Galoisy and Calas, 1991). Although the contribution of  $^{55}Ni$  and  $^{64}Ni$  varies among the spectra, the energy of the optical transitions remains the same, which indicates that Ni is distributed between two sites of constant geometry.

In the  $K_2NiSi_3O_8$  glass, EXAFS indicates the presence of four Si second neighbors, which is consistent with Ni

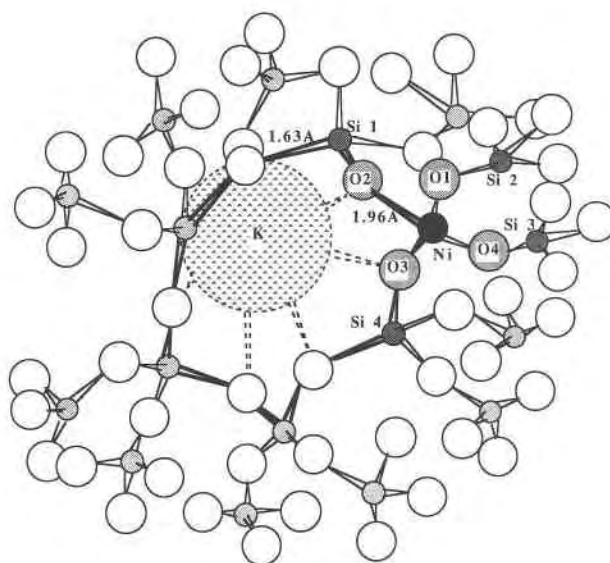


Fig. 4. Model of the  $^{64}Ni$  environment in  $K_2NiSi_3O_8$  glass showing the contribution of the  $NiO_4$  tetrahedron to the glassy network.

belonging to the silicate network (Fig. 4). However, the charge-compensation process has not been revealed by our EXAFS data, even at  $77\text{ K}$ , probably because of the strong static disorder that affects the position of the weakly bonded alkalis. The intertetrahedral  $^{64}Ni$ -O-Si angle ( $\alpha$ ) of  $127 \pm 5^\circ$  has been calculated from the EXAFS-derived Ni-O and Ni-Si distances, assuming a mean Si-O bond length of  $1.63\text{ \AA}$  as in similar glasses (Navrotsky et al., 1985). This angle is reduced by about  $15^\circ$  as compared with the Si-O-(Al,Si) angle determined in  $NaAlSi_3O_8$  and  $KAlSi_3O_8$  glasses of  $143$  and  $146^\circ$ , respectively (Taylor and Brown, 1979). This shows that Si-O-T angle decreases with the formal charge of tetrahedral cation T and hence with weaker nonbonded Si-T repulsions (O'Keefe and Hyde, 1981). As optical transitions of  $^{64}Ni$  occur at the same energy in  $K_2NiSi_3O_8$  and  $Na_2NiSi_3O_8$  glasses,  $\alpha$  has the same value in both glasses. The weak peak observed near  $2.7\text{ \AA}$  in the FT of the  $CaNiSi_2O_6$  glass (Galoisy and Calas, 1991) may also correspond to the same contribution.

The field strength of the charge-compensating alkali ( $M$ ) may explain the differences of the Ni environment in the glasses investigated. The higher the cation field strength, the less efficient the charge compensation, as observed in  $SiO_2$ - $MAIO_2$  glasses (Navrotsky et al., 1985). Ni is the first element case where the competition between depolymerization and charge compensation in silicate glasses is evident. Small divalent cations may be part of the tetrahedral framework, provided weakly polarizing cations exist for charge compensation, but if this possibility does not occur, divalent cations occur in a distinct environment. The information drawn from XAS and optical spectroscopy is that these two environments are well defined and rather constant among silicate glasses. This

confirms also the heterogeneous structure of silicate glasses, shown by recent neutron scattering data on calcium and nickel silicate glasses determined using isotope substitution (Gaskell et al., 1991, 1992). Because of the similar crystal chemical properties of Mg and Ni, Mg may show the same coordination states as Ni in glasses. Crystalline analogues with leucite and pollucite structures show indeed the possibility for divalent cations such as Mg or Fe to be part of a silicate framework (see Kohn et al., 1991). This raises the possibility of a change in the cation environment with pressure, higher coordination numbers being favored by higher pressures, as shown in germanate glasses using high-pressure dispersive EXAFS (Itié et al., 1989). Such coordination changes might strongly affect the geochemistry of these elements in the mantle. Our results also seem to indicate that the glass stoichiometry does not warrant a defined glass structure, since the stoichiometry relies on an assumption concerning the O coordination state. Despite its feldspar-like composition, the  $\text{NaNiSi}_3\text{O}_8$  glass does not have a framework structure. However, XAS did not show such a difference in the environment of  $\text{Fe}^{2+}$  in ferrous equivalent glasses, nor did  $^{57}\text{Fe}$  show any clear relation with the silicate network (Waychunas et al., 1988).

The presence of two dissimilar sites occupied by Ni in silicate melts and glasses is of importance for understanding the geochemistry of this element, a point first raised by Burns and Fyfe (1964). The strong variations observed in the distribution of Ni among these sites as a function of the glass and melt composition explain the chemical dependence of partition coefficients, as Ni is less stabilized in tetrahedral than in pentahedral sites (Galoisy and Calas, in preparation). The strong enrichment of Ni in olivines coexisting with potassic melts (Takahashi, 1978) supports this conclusion.

#### ACKNOWLEDGMENTS

We are grateful to Aline Ramos and the staff of LURE (Orsay) for their help in XAS measurements. We also thank G.E. Brown and P.H. Gaskell for fruitful discussions. This work was supported by the CNRS/INSU "Dynamique et Bilan de la Terre" Program (Contribution CNRS/DBT no. 451).

#### REFERENCES CITED

- Burns, R.G. (1970) Mineralogical applications of crystal field theory. Cambridge University Press, Cambridge, U.K.
- Burns, R.G., and Fyfe, W. (1964) Site of preference energy and selective uptake of transition-metal ions from a magma. *Science*, 144, 1001–1003.
- Calas, G., and Petiau, J. (1983) Structure of oxide glasses. Spectroscopic studies of local order and crystallochemistry. *Geochemical implications*. *Bulletin de Minéralogie*, 106, 33–55.
- Cartier, C., and Verdaguer, M. (1989) Structures fines d'absorption des

- rayons X: Étude au seuil K de complexes moléculaires de métaux de transition. *Journal de Chimie Physique*, 86, 1607–1621.
- Eisenberger, P., and Brown, G.S. (1979) The study of disordered systems by EXAFS: Limitations. *Solid State Communications*, 29, 481–484.
- Galoisy, L., and Calas, G. (1991) Spectroscopic evidence for five-coordinated Ni in  $\text{CaNiSi}_2\text{O}_6$  glass. *American Mineralogist*, 76, 1777–1780.
- Galoisy, L., Calas, G., and Maquet, M. (1991) Alumina fused cast refractory ageing monitored by nickel crystal chemistry. *Journal of Materials Research*, 6, 2434–2441.
- Gaskell, P.H., Esckersley, M.C., Barnes, A.C., and Chieux, P. (1991) Medium range order in the cation distribution of a calcium silicate glass. *Nature*, 350, 675–677.
- Gaskell, P.H., Zhao, J., Calas, G., and Galoisy, L. (1992) The structure of mixed cation oxide glasses. In L.D. Pye, W.C. LaCourse, and H.V. Stevens, Eds., *Physics of non-crystalline solids*, vol. VII, p. 53–58. Taylor and Francis, New York.
- Hart, S.R., and Davis, K.E. (1978) Nickel partitioning between olivine and silicate melt. *Earth and Planetary Science Letters*, 40, 203–220.
- Itié, J.P., Polian, A., Calas, G., Petiau, J., Fontaine, A., and Tolentino, H. (1989) Pressure-induced coordination changes in crystalline and vitreous  $\text{GeO}_2$ . *Physical Review Letters*, 63, 398–401.
- Kinzler, R.J., Grove, T.L., and Recca, S.I. (1990) An experimental study on the effect of temperature and melt composition on the partitioning of nickel between olivine and silicate melt. *Geochimica et Cosmochimica Acta*, 54, 1255–1265.
- Kohn, S.C., Dupree, R., Mortuza, M.G., and Henderson, C.M.B. (1991) An NMR study of structure and ordering in synthetic  $\text{K}_2\text{MgSi}_5\text{O}_{12}$ , a leucite analogue. *Physics and Chemistry of Minerals*, 18, 144–152.
- Lemarchand, F., Villemant, B., and Calas, G. (1987) Trace element distribution coefficients in alkaline series. *Geochimica et Cosmochimica Acta*, 51, 1071–1081.
- Manceau, A., and Calas, G. (1986) Nickel-bearing clay minerals. 2. Intracrystalline distribution of nickel: A spectroscopic study. *Clay Minerals*, 21, 341–360.
- McKale, A.G., Veal, B.W., Paulikas, A.P., Chan, S.K., and Knapp, G.S. (1988) Improved ab initio calculations of amplitude and phase functions for extended X-ray absorption fine structure spectroscopy. *Journal of the American Chemical Society*, 110, 3763–3768.
- Navrotsky, A., Geisinger, K.L., McMillan, P., and Gibbs, G.V. (1985) The tetrahedral framework in glasses and melts. Inferences from molecular orbital calculations and implications for structure, thermodynamics, and physical properties. *Physics and Chemistry of Minerals*, 11, 284–298.
- Nelson, C., Furukawa, T., and White, W.B. (1983) Transition metal ions in glasses: Network modifiers or quasi-molecular complexes? *Materials Research Bulletin*, 18, 959–966.
- O'Keefe, M., and Hyde, B.G. (1981) The role of non-bonded forces in crystals. *Structure and Bonding in Crystals*, 1, 227–254.
- Sakurai, T., Ishigame, M., and Arashi, H. (1969) Absorption spectrum of  $\text{Ni}^{2+}$  ions in spinel. *Journal of Chemical Physics*, 50, 3241–3245.
- Takahashi, E. (1978) Partitioning of  $\text{Ni}^{2+}$ ,  $\text{Co}^{2+}$ ,  $\text{Fe}^{2+}$ ,  $\text{Mn}^{2+}$  and  $\text{Mg}^{2+}$  between olivine and silicate melts: Compositional dependence of partition coefficients. *Geochimica et Cosmochimica Acta*, 42, 1829–1844.
- Taylor, M., and Brown, G.E., Jr. (1979) Structure of mineral glasses—I. The feldspar glasses  $\text{NaAlSi}_3\text{O}_8$ ,  $\text{KAlSi}_3\text{O}_8$ ,  $\text{CaAl}_2\text{Si}_2\text{O}_8$ . *Geochimica et Cosmochimica Acta*, 43, 61–75.
- Waychunas, G.A., Brown, G.E., Ponader, C.W., and Jackson, W.E. (1988) Evidence from X-ray absorption for network-forming  $\text{Fe}^{2+}$  in molten silicates. *Nature*, 332, 251–253.

MANUSCRIPT RECEIVED MARCH 11, 1992

MANUSCRIPT ACCEPTED APRIL 14, 1992